Faraday Discussions

Accepted Manuscript

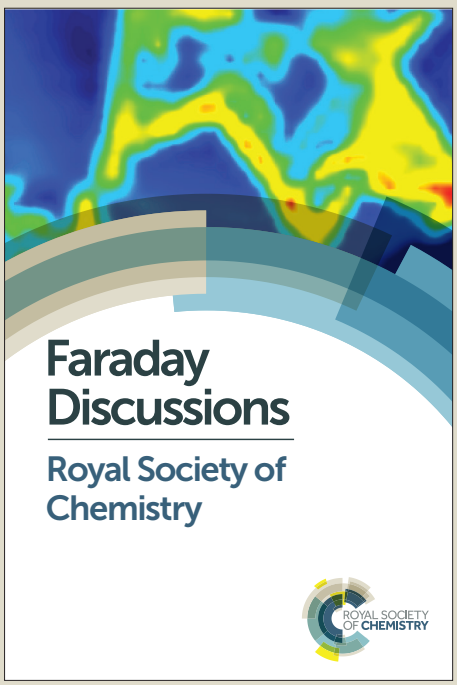

This article can be cited before page numbers have been issued, to do this please use: M. Tagliazucchi and I. Szleifer, *Faraday Discuss.*, 2015, DOI: 10.1039/C5FD00115C.

ROYAL SOCIETY OF CHEMISTRY

www.rsc.org/faraday_d

View Article Online
DOI: 10.1039/C5FD00115C

Faraday Discussions

ARTICLE

Received 00th January 20xx,

Accepted 00th January 20xx

DOI: 10.1039/x0xx00000x

www.rsc.org/

Dynamics of Dissipative Self-Assembly of Particles Interacting through Oscillatory Forces

M. Tagliazucchi[a,b] and I. Szleifer[a]

Dissipative self-assembly is the formation of ordered structures far from equilibrium, which continuously uptake energy and dissipate it into the environment. Due to its dynamical nature, dissipative self-assembly can lead to new phenomena and possibilities of self-organization that are unavailable to equilibrium systems. Understanding the dynamics of dissipative self-assembly is required in order to direct the assembly to structures of interest. In the present work, Brownian Dynamics simulations and analytical theory were used to study the dynamics of self-assembly of a mixture of particles coated with weak acids and bases under continuous oscillations of pH. The pH of the system modulates the charge of the particles and, therefore, the interparticle forces oscillate in time. This system produces a variety of self-assembled structures, including colloidal molecules, fibers and different types of crystalline lattices. The most important conclusions of our study are: i) in the limit of fast oscillations, the whole dynamics (and not only the non-equilibrium steady-state) of a system of particles interacting through time-oscillating interparticle forces can be described by an effective potential that is the time average of the time-dependent potential over one oscillation period. ii) The oscillation period is critical to determine the order of the system. In some cases order is favored by very fast oscillations while in others cases small oscillation frequencies increase order. In the latter case, it is shown that slow oscillations remove kinetic traps and, thus, allow the system to evolve towards the most stable non-equilibrium steady-state.

Introduction

Colloidal self-assembly is a topic of both fundamental interest and practical relevance. Colloids are unique and versatile tools to study important problems in self-assembly, such as the effect of shape and directional interactions,[1-7] symmetry breaking,[8] kinetic versus thermodynamic control,[9, 10] the role of entropy[1, 7, 11-14] and far-from-equilibrium self-organization.[8, 15-21] Further, developments in colloidal self-assembly enable new avenues for the fabrication of nanoparticle-based devices for applications in electronics,[22, 23] batteries,[24] photodetectors,[25] photonics[3, 26] and bioanalysis.[27] The great majority of experimental and theoretical work in the area of colloidal self-assembly is focused on equilibrium systems. However, there is a recent and widespread interest in self-organization far from thermodynamic equilibrium. Far-from-equilibrium self-organization, also known as dissipative self-assembly,[16] requires a continuous influx of energy into the system and energy dissipation by the system into its surroundings. While equilibrium colloidal self-assembly is relatively well understood, we still know very little about the rules that govern dissipative self-assembly as well as its potential advantages and limitations.[28] Here, we build on our previous work on dissipative self-assembly via the oscillation of interparticle interactions[20] and provide new insights about the dynamics of this process.

In dissipative self-assembly, the particles in the system couple to a source of energy that keeps the system far from equilibrium. This coupling can be either invariant in time or periodically modulated. Examples of systems where the coupling remain invariant in time are colloidal spinners driven by a constant torque,[19, 29] charged particles in constant electric fields[8, 18] and particles that self-propel with a constant force.[15, 21, 30] On the other hand, when the coupling between the system and the energy source is periodically modulated, some external or internal variable must oscillate in time, such as the strength of the interactions between particles[17, 20, 31-33] or the magnitude and direction of an external field.[5, 7, 16, 34-37] In these cases, the system evolves in time toward a non-equilibrium steady-state (NESS) that is oscillatory in nature: the properties of the system in the NESS are equivalent at time t and at time $t+\tau$ (where τ is the oscillation period).

Dissipative systems may have more than one NESS,[38] so an important and open question is how to control the evolution of these systems toward a specific NESS. This problem is, of course, analog to the problem of finding the conditions that direct the evolution of equilibrium self-assembly toward a determined local minimum of the free-energy. However, dissipative systems involve an additional level of complexity

[a] Department of Biomedical Engineering, Department of Chemistry and Chemistry of Life Processes Institute, Northwestern University, Evanston, IL 60208 (USA)..
[b] INQUIMAE-CONICET, Ciudad Universitaria, Pabellón 2, Ciudad Autónoma de Buenos Aires C1428EHA (Argentina)..

† Electronic Supplementary Information (ESI) available. See DOI: 10.1039/x0xx00000x

ARTICLE View Article Online Journal Name DOI: 10.1039/C5FD00115C

due to the lack of variational principles, such as the minimization of free energy that rules equilibrium systems.

In the present work, we explore the dynamics of a dissipative system of particles interacting through oscillatory forces as they evolve toward a NESS. Our model dissipative system, introduced in our previous work,[20] is a mixture of colloids under periodic pH oscillations, where half of the particles are coated by weak acids and the other half by weak bases. We analytically prove here that the whole dynamics of dissipative self-assembly in the limit of fast oscillations is described by an effective potential that is the time average of the oscillatory potential. We numerically confirm this result showing that two systems that have different oscillatory potentials, but the same effective potential, exhibit the same dynamics in the limit of fast oscillations. Finally, we examine the effect of the oscillation period on the dynamics and outcome of dissipative self-assembly and show that in some cases order is favored by fast oscillations, but in others slow oscillations increase the homogeneity of the system by allowing particles to escape from kinetic traps.

Theoretical Methods

We studied the dissipative self-assembly of particles interacting through oscillatory potentials in a mixture of colloids coated by weak acids functionalities (*a*-type particles) and colloids coated by weak basic functionalities (*b*-type particles) under continuous oscillations of the solution pH. The charge of *a*-type and *b*-type particles change with pH according to the acid-base equilibrium of the charged groups on their surfaces. Neglecting charge regulation effects,[39-41] the charges of the particles are determined by the expressions for the acid base equilibria, i.e.

$$z_a = -z_0 \frac{1}{1+10^{-(pH-pKa)}} \quad (1)$$

for *a*-type particles and

$$z_b = z_0 \frac{1}{1+10^{(pH-pKa)}} \quad (2)$$

for *b*-type particles. For simplicity, we use here the same maximum absolute charge (z_0) and p*Ka* (p*Ka* = 5) for both types of particles. Figure 1A shows a plot of the charge of the particles as the pH is varied from 3 to 7 and back to 3. For pH = 3, *a*-type particles are almost neutral and *b*-type particles have a charge of z_0. For pH = p*Ka* = 5, *a*-type particles have a charge of -½·z_0 and *b*-type particles have a charge of ½·z_0. Finally, for pH = 7, *a*-type have a charge of $-z_0$ and *b*-type particles are almost neutral. We oscillate the pH of the system with a period τ using either a triangular (Figure 1B) or a sawtooth (Figure 1C) pH-time program, see below. We also explore in this work the situation where the pH is oscillated between 3 and 5 with a triangular program, Figure 1D.

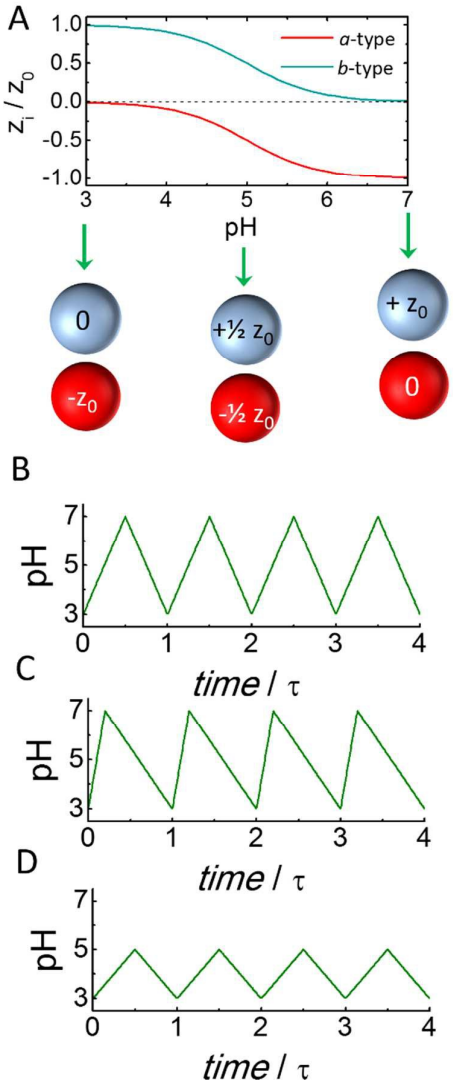

Figure 1: A. Charge of *a*-type and *b*-type particles as a function of the solution pH (determined with equations (1) and (2). In this work, the pH was oscillated in time between pH 3 and pH 7 following a linear triangular (B) or sawtooth (C) program or between 3 and 5 with a triangular program (D).

We model the evolution of the system using Brownian Dynamics (BD) in a 2D box with periodic boundary conditions. The equation of motion in BD is:

$$-\frac{d\mathbf{r}_i}{dt}\xi + \sqrt{2\xi k_B T}\,\mathbf{R}_i(t) - \nabla u_i(\mathbf{r}_i) = 0 \quad (3)$$

where r_i and u_i are the position and potential energy of particle *i*, respectively; ξ is the drag coefficient and $\mathbf{R}_i(t)$ is a Gaussian random force acting on particle *i* with components $R_{ij}(t)$ that have zero mean, $\langle R_{ij}(t)\rangle = 0$, and delta-function correlation, $\langle R_{ij}(t)\cdot R_{ij}(t')\rangle = \delta(t-t')$. The drag coefficient is related to the particle diffusion coefficient and diameter (σ) and the solvent viscosity (η) by,

$$\xi = \frac{k_B T}{D} = 3\pi\eta\sigma \quad (4)$$

Journal Name

View Article Online
ARTICLE
DOI: 10.1039/C5FD00115C

Equation (3) is similar to the Langevine equation,[42] but neglecting the inertial term as the characteristic inertial timescale is much smaller than the diffusional timescale. The first two terms in equation (3) model the friction of the solvent and the random collisions of its molecules with the particles, respectively. The last term in equation (3) models the conservative forces. For simplicity, we neglect the hydrodynamic forces between the particles and between the particles and the substrate.

The interparticle potential is pairwise-additive and results from the combination of a screened electrostatic potential and a short-range repulsive potential (we neglect many body effects[43]). Since the ions are considered implicitly in our system, the interaction between particles is modeled with a Yukawa potential, which describes electrostatic interactions screened by mobile ions,

$$u_{ij}^{Yuk}(r) = \frac{z_i}{z_0}\frac{z_j}{z_0}\frac{C}{r}\mathrm{e}^{-\frac{r}{\lambda_D}} \quad (5)$$

In equation (5), λ_D is the solution Debye length (we used λ_D = 1.5σ in all calculations) and *C* is a constant that determines the strength of the electrostatic potential in the system, given by

$$C = \frac{4z_0^2 e^{\frac{\sigma}{\lambda_D}}\lambda_B}{\left(2+\kappa\sigma\right)^2} \quad (6)$$

where λ_B is the Bjerrum length. The short-range repulsions are modeled using the repulsive component of the Lennard-Jones potential,

$$u_{ij}^{rep}(r) = \left(\frac{\sigma}{r}\right)^{12} \quad (7)$$

Finally, we cut-off and shift the total interparticle as:

$$u_{ij}(r) = \begin{cases} u_{ij}^{rep}(r) + u_{ij}^{Yuk}(r) - \left[u_{ij}^{rep}(r_{cutoff}) + u_{ij}^{Yuk}(r_{cutoff})\right] & \text{for } r < r_{cut-off} \\ 0 & \text{for } r \geq r_{cut-off} \end{cases} \quad (8)$$

We use a long cut-off radius $r_{\text{cut-off}}$ of 8σ in order to assure $u_{ij}^{rep}(r_{cutoff}) + u_{ij}^{Yuk}(r_{cutoff}) < 0.05 k_B T$ for all conditions studied.

We performed BD simulations in two dimensions with a home-developed parallel code that allows modifying the interparticle potential in each time step. In all cases, we simulated 2500 particles and started from a disordered system of particles interacting only through repulsive LJ potentials. The simulation time step was 10^{-6} t_d.

We use dimensionless variables: lengths are normalized by the diameters of the colloids, σ, and times by the characteristic diffusion timescale, $t_d = \sigma^2/D$ (where *D* is the particle diffusion coefficient). In the Supporting Information of our previous work,[20] we discussed the conversion from dimensionless units to real units and showed that dissipative self-assembly of particles with diameters of 10 nm to 1 μm would require oscillation periods of microseconds to seconds.

Results and Discussion

Dissipative Self-Assembled Structures

In our previous work,[20] we performed a systematic investigation of the self-assembled morphologies that form upon pH oscillations in a system with equal number of *a*-type and *b*-type particles. Figure 2 shows the morphologies reported in our previous work and additional morphologies that result from changing the ratio of *a*-type to *b*-type particles. All these morphologies were obtained in the limit of very fast oscillations ($\tau \to 0$).

The dimers are the predominant structure for a 1:1 composition at density ρ = 0.11 *part*·σ^{-2}. However, under these conditions we also observe the formation of a few trimers (both a_2b and ab_2) as well as isolated *a* and *b* particles. Increasing the fraction of *a*-type particles to 2:1 produces a_2b trimers (again with some *a*, *b* and *ab* impurities). Interestingly, increasing the *a*:*b* ratio beyond 2:1 does not produce colloidal molecules with more than two *a*-type particles per *b*-type particle (i.e. we do not obtain a_3b, a_4b, *etc*). We will show below that such colloidal molecules are unstable when the pH is oscillated between 3 and 7, but they can form by oscillating the pH between 3 and 5.

For ρ = 0.39 *part*·σ^{-2} and *a*:*b* = 1:1, we observe fibers formed by the head-to-tail association of dimers. For ρ = 1.0 *part*·σ^{-2}, we observe crystalline lattices for *a*:*b* = 1:1 and 2:1. Even though these crystals have a large number of defects, it is possible to identify their unit cell, whose composition is equal to the global composition of the system. For *a*:*b* = 1:1, we obtain a honeycomb structure with an hexagonal unit cell (already reported in our previous work[20]). For *a*:*b* = 2:1, the system forms an open square lattice.

Finally, for ρ = 1.56 *part*·σ^{-2}, the system is compressed beyond the density required to close pack hard disks with diameter σ (1.15 *part*·σ^{-2}). In these conditions (which are not experimentally achievable but are discussed here for completeness) we observe the formation of a square lattice (with a small hexagonal distortion) for *a*:*b* = 1:1, as was reported in our previous work.[20]

ARTICLE View Article Online Journal Name DOI: 10.1039/C5FD00115C

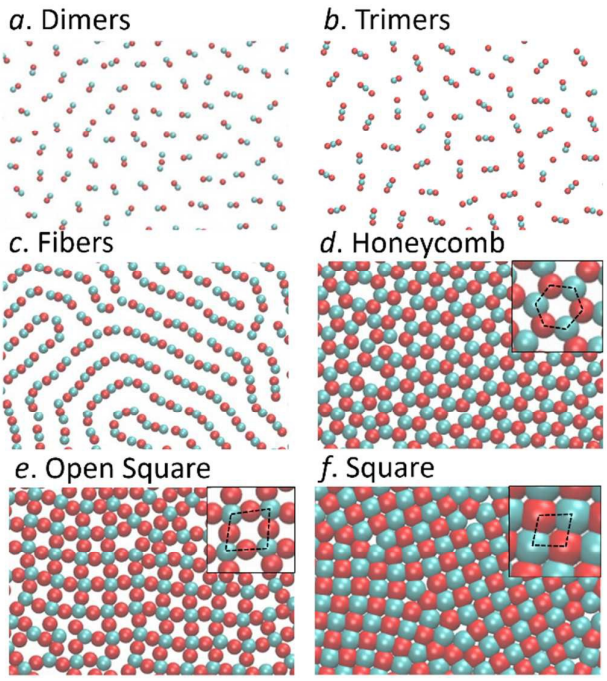

Figure 2: Morphologies of the dissipative self-assembled systems. The snapshots show the morphologies obtained in the limit of very fast oscillations ($\tau \to 0$, obtained using an effective potential, see below), C = 1000 k_BT·σ, a triangular pH-time program (Figure 1B) and the following densities and compositions: dimers, ρ = 0.11 *part*·σ^{-2} and *a*:*b* = 1:1; trimers, ρ = 0.11 *part*·σ^{-2} and *a*:*b* = 2:1; fibers, ρ = 0.39 *part*·σ^{-2} and *a*:*b* = 1:1; honeycomb, ρ = 1.0 *part*·σ^{-2} and *a*:*b* = 1:1; open squares, ρ = 1.0 *part*·σ^{-2} and *a*:*b* = 2:1; square, ρ = 1.56 *part*·σ^{-2} and *a*:*b* = 1:1. Only part of the simulation box is shown. The diameter of the colloids is σ in all cases; red and blue particles represent *a*-type and *b*-type particles, respectively. In the cases where the system forms a periodic lattice, we show the unit cell of the lattice as an inset in the upper right corner of the panel.

Analytical Analysis of the Dynamical Evolution of Particles Interacting through Oscillatory Potentials in the Limit of Fast Oscillations.

In our previous work,[20] we demonstrated that the non-equilibrium steady state (NESS) of a system of particles interacting through oscillatory forces in the limit of very fast oscillations is equivalent to the equilibrium state of a system of particles interacting via a non-oscillatory effective potential. In that demonstration, we used a power series expansion of the Fokker-Planck equation in terms of τ, the period of the oscillation. We now use a different approach in order to prove a more general result: we show here that the effective potential describes the full kinetics of the non-equilibrium systems for very fast oscillations (not only for the NESS), i.e. the effective potential describes the whole dynamics of the system as it approaches its NESS.

We start by writing down the Fokker-Planck equation for the system,[42]

$$\frac{\partial p(\mathbf{r},t)}{\partial t} = \hat{L}p(\mathbf{r},t) \tag{9}$$

where $p(\mathbf{r}, t)$ is the probability density at time t, i.e. the probability to find the system at **r** (where **r** is the vector of the positions of all particles in the system) at time t. The Fokker-Planck operator $\hat{L}$ is defined as:

$$\hat{L}p(\mathbf{r},t) = D\nabla\left(\nabla p(\mathbf{r},t) + p(\mathbf{r},t)\nabla U(\mathbf{r},t)\right) \tag{10}$$

where $U(\mathbf{r}, t)$ is the potential energy of the system. We will consider the evolution of the system during the period of an oscillation, τ. Let us first assume that there exists a time-independent effective potential, U_{eff}, that describes the evolution of the system. In that case, U (and therefore $\hat{L}_{eff}$) are time-independent and thus there is a formal solution for equation (9), which is given by,[32]

$$p(\mathbf{r},t+\tau) = \exp\left(\tau\hat{L}_{eff}\right)p(\mathbf{r},t) \tag{11}$$

Here, $\hat{L}_{eff}$ is the time-independent effective Fokker-Planck operator. Expanding the exponential as a power series of $\tau\cdot\hat{L}_{eff}$ results in:

$$p(\mathbf{r},t+\tau) = \left(1+\tau\hat{L}_{eff}+\frac{1}{2!}\tau^2\hat{L}_{eff}^{\ 2}+\ldots\right)p(\mathbf{r},t) \tag{12}$$

Let us now focus on the system of particles interacting through oscillatory forces. In that case, U and $\hat{L}$ depend on time and thus equation (11) is no longer a solution of the Fokker-Planck equation. However, we can divide the oscillation period τ in infinitesimally small time steps $dt = \tau/N$, such that U and $\hat{L}$ are time-independent within each time step. We then propagate the probability density from t to $t + \tau$ using these small time steps:

$$\begin{aligned} &p(\mathbf{r},t+\tau) = \\ &\exp\left(dt\cdot\hat{L}\left(t+Ndt\right)\right)\ldots\exp\left(dt\cdot\hat{L}\left(t+dt\right)\right)p(\mathbf{r},t) \\ &= \prod_{j=1,N}\exp\left(\left(\tau/N\right)\cdot\hat{L}\left(t+j\tau/N\right)\right)p(\mathbf{r},t) \end{aligned} \tag{13}$$

Expanding the exponentials as power series yield,

$$p(\mathbf{r},t+\tau) = \prod_{j=1,N}\left(1+\left(\tau/N\right)\cdot\hat{L}\left(t+j\tau/N\right)+\frac{1}{2!}\left(\tau/N\right)^2\cdot\hat{L}\left(t+j\tau/N\right)^2+\ldots\right)p(\mathbf{r},t) \tag{14}$$

We expand the multiplications and group terms of same power in τ,

Journal Name

View Article Online
ARTICLE
DOI: 10.1039/C5FD00115C

$$p(\mathbf{r},t+\tau)=\left(1+\tau\sum_{j=1,N}\frac{1}{N}\cdot\hat{L}\left(t+j\tau/N\right)+\right.$$
$$\left.\tau^2\cdot\left[\sum_{j=1,N}\left(\frac{\hat{L}\left(t+j\tau/N\right)}{N}\sum_{i=j,N}\frac{\hat{L}\left(t+i\tau/N\right)}{N}\right)-\frac{1}{2}\sum_{j=1,N}\frac{\hat{L}\left(t+j\tau/N\right)^2}{N^2}\right]+\ldots\right)p(\mathbf{r},t) \quad (15)$$

The terms of order τ^2 in eq. (15) cannot be factorized as the square of a summation due to the fact that $\hat{L}(t)$ and $\hat{L}(t')$ do not commute for $t \neq t'$ because U depends on t.

We define $h = j/N$, $k = i/N$, $dh = dk = 1/N$ and take the limit $dt \to 0$ and $N \to \infty$,

$$p(\mathbf{r},t+\tau)=\left(1+\tau\int_0^1 dh\hat{L}\left(t+\tau h\right)+\right.$$
$$\left.\tau^2\left[\int_0^1 dh\hat{L}\left(t+\tau h\right)\int_h^1 dk\hat{L}\left(t+\tau k\right)\right]+\ldots\right)p(\mathbf{r},t) \quad (16)$$

We note that

$$\left(\int_0^1 dh\hat{L}\left(t+\tau h\right)\right)p\left(\mathbf{r},t\right)=$$
$$D\nabla\left(\nabla p\left(\mathbf{r},t\right)+p\left(\mathbf{r},t\right)\nabla\left(\int_0^1 U\left(\mathbf{r},t+\tau h\right)dh\right)\right)$$
$$=D\nabla\left(\nabla p\left(\mathbf{r},t\right)+p\left(\mathbf{r},t\right)\nabla U_{eff}\left(\mathbf{r}\right)\right) \quad (17)$$

where $U_{eff}(r)$ is the average of the potential energy of the system over one oscillation period, i.e.

$$U_{eff}\left(\mathbf{r}\right)=\int_0^1 U\left(\mathbf{r},t+\tau h\right)dh \quad (18)$$

Note that since $U(r,t)$ is a periodic function with period τ, $U_{eff}(r)$ does not depend on t. Equation (17) suggests the convenience of defining the operator,

$$\hat{L}_{eff}\,p\left(\mathbf{r},t\right)=D\nabla\left(\nabla p\left(\mathbf{r},t\right)+p\left(\mathbf{r},t\right)\nabla U_{eff}\left(\mathbf{r}\right)\right) \quad (19)$$

and rewrite eq. (16) in terms of this operator:

$$p(\mathbf{r},t+\tau)=\left(1+\tau\hat{L}_{eff}+\right.$$
$$\left.\tau^2\left[\int_0^1 dh\hat{L}\left(t+\tau h\right)\int_h^1 dk\hat{L}\left(t+k\tau\right)\right]+\ldots\right)p(\mathbf{r},t) \quad (20)$$

Comparison between equations (12) and (20) shows that these two equations agree up to first order in τ. In other words, the whole evolution of the system of particles interacting via oscillatory potentials can be described in terms of a system of particles interacting through an effective non-oscillatory potential U_{eff} only when the terms of second order and greater in τ can be neglected in eq. (20). This is the limit of very fast oscillations, $\tau \to 0$. Note that we did not require non-equilibrium steady-state (NESS) conditions in this derivation (unlike the derivation in our previous work[20]), therefore, we proved that the effective non-oscillatory potential can be used to describe the whole dynamics of the oscillatory system (and not only the NESS) in the limit of fast oscillations.

If only pairwise interactions are present, the effective potential is given by,

$$U_{eff}=\frac{1}{2}\sum_{i=1}^{N}\sum_{j=1}^{N}u_{ij}^{eff} \quad (21)$$

where u_{ij}^{eff} is the effective potential between particles i and j. In the present example, the interparticle potential is a combination of a short-range LJ repulsion and a screened electrostatic interaction (Yukawa potential). The pH oscillations affect the charge of the particle and, therefore, the screened electrostatic potential changes in time, but the repulsive part of the potential is time-independent. The effective potential, therefore, is

$$u_{ij}^{eff}(r)=\left\langle u_{ij}^{rep}(r)\right\rangle+\left\langle u_{ij}^{Yuk}(r)\right\rangle=$$
$$u_{ij}^{rep}(r)+\frac{\left\langle z_i\cdot z_j\right\rangle}{{z_0}^2}\frac{C}{r}\mathrm{e}^{-\frac{r}{\lambda_D}} \quad (22)$$

where $\langle\ldots\rangle=\frac{1}{\tau}\int_t^{t+\tau}\ldots dt$ and we omitted the cut-off scheme for simplicity. The effective potential is, hence, dictated by the factor $\left\langle z_i\cdot z_j\right\rangle$, whose exact value depends on the shape of the pH-time program. The potentials in Figures 1B (linear triangular potential) and 1C (linear saw-tooth potential) have the same values of $\left\langle z_i\cdot z_j\right\rangle$ because the value of $\left\langle z_i\cdot z_j\right\rangle$ when the pH is linearly ramped from 3 to 7 is equal to that when the pH linearly decreases from 7 to 3 and it does not depend on the rate at which the pH changes. Therefore, according our analytical results, the two potential programs in Figures 1B and 1C should produce the same dynamics and non-equilibrium steady-state in the limit $\tau \to 0$. We show next simulation results that confirm this prediction.

Simulation of the Dynamical Evolution of Particles Interacting through Oscillatory Potentials in the Limit of Fast Oscillations

Figure 3A shows the time evolution of the average bond-order parameter of order 2, $\overline{\psi}_2$, as a function of the simulation time for the formation of fibers (a:b = 1:1, ρ = 0.39 *part*·σ^{-2}). We define the average bond-order parameter of order n as,

ARTICLE View Article Online Journal Name DOI: 10.1039/C5FD00115C

$$\bar{\psi}_n(t) = \frac{1}{N_{part}} \sum_{j=1}^{N_{part}} \psi_n(j,t) \quad (23)$$

where N_{part} is the total number of particles and $\psi_n(j,t)$ is the bond-order parameter of particle j at time t, which we define as,[44-46]

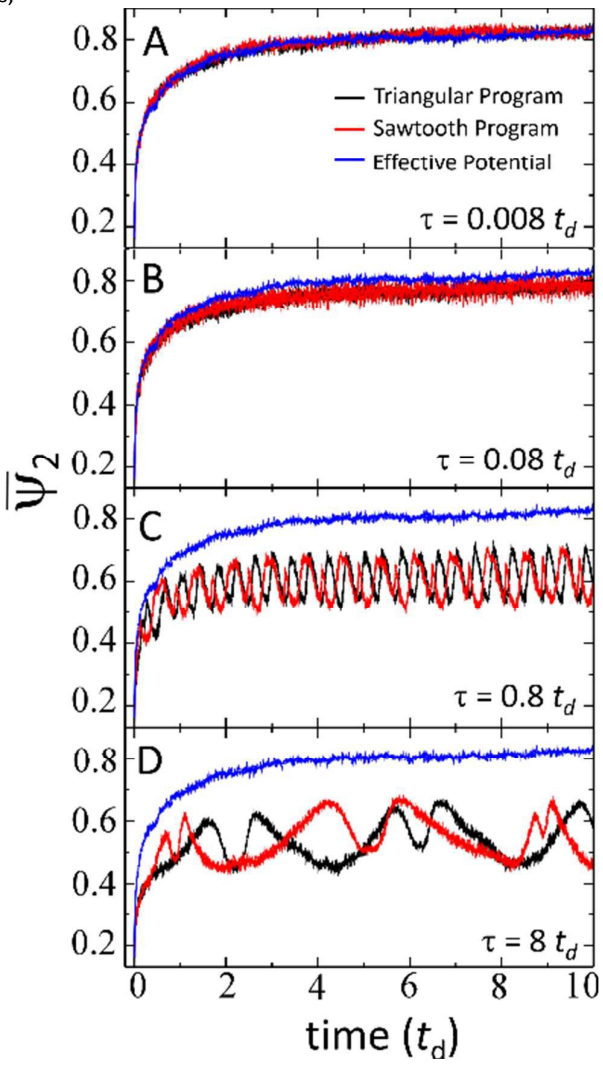

Figure 3: Bond-order parameter of order 2 ($\bar{\psi}_2$) as a function of simulation time for a:b = 1:1, ρ = 0.39 *part*·σ^{-2} and C = 1000 k_BT·σ and an oscillation period τ of (A) 0.008, (B) 0.08, (C) 0.8 and (D) 8 t_d. Values of $\bar{\psi}_2$ close to one indicate the formation of a well-ordered fiber morphology. Black and red lines show the results of simulations where the pH was varied with the triangular program (shown in Figure 1B) and the sawtooth program (shown in Figure 1C), respectively. Blue lines show the result of a simulation using the effective potential given by equation (22) (this result is independent of τ and, thus, the same curve is shown in all panels).

$$\psi_n(j,t) = \begin{cases} \left| \frac{1}{NN(j)} \sum_{k=1}^{NN(j)} \exp\left(n\theta_{jk}(t)i\right) \right| & \text{for } NN(j) \geq n \\ 0 & \text{for } NN(j) < n \end{cases} \quad (24)$$

where $i = \sqrt{-1}$, $NN(j)$ is the number of nearest neighbors of the particle j within a distance of 1.5·σ and θ_{jk} is the angle between the vector formed by the centers of particle j and k and a fixed (arbitrary) axis. The order parameter $\psi_n(j,t)$ has a maximum value of one when particle j has n neighbours separated by angles of $2\pi/n$. Therefore, the fiber structure is well characterized by the order-parameter of order two: the larger $\bar{\psi}_2$, the closer the system is to a perfect straight fiber.

The black and red lines in Figure 3A show the time-evolution of $\bar{\psi}_2$ for a simulation where the pH was oscillated with the triangular linear program (Figure 1B) and the sawtooth linear program (Figure 1C), respectively. In this panel, the oscillation period (τ = 0.008 t_d) was much smaller than the characteristic diffusional time-scale of the system (t_d). The blue line shows the results of a simulation performed with the time-independent effective potential given by equation (22). As we already mentioned, both the triangular and the sawtooth linear programs have exactly same effective potential. We observe that, in the limit of fast oscillations, the $\bar{\psi}_2$ vs time curves for the triangular program, the sawtooth program and the effective potential overlap, as predicted by our analytical results. Note that the degree of agreement of the $\bar{\psi}_2$ vs time curves decreases as the frequency of the oscillation decreases (Figures 3B, 3C and 3D). Figure 4 shows snapshots of the system for the triangular and sawtooth potentials at a simulation time of 4 t_d for τ = 0.008 t_d and 8 t_d. For τ = 8 t_d, the morphologies produced by the triangular and the sawtooth potentials are very different. However, both pH-time programs yield well-ordered fibers for τ = 0.008 t_d, in agreement with the results in Figure 3 and our analytical predictions.

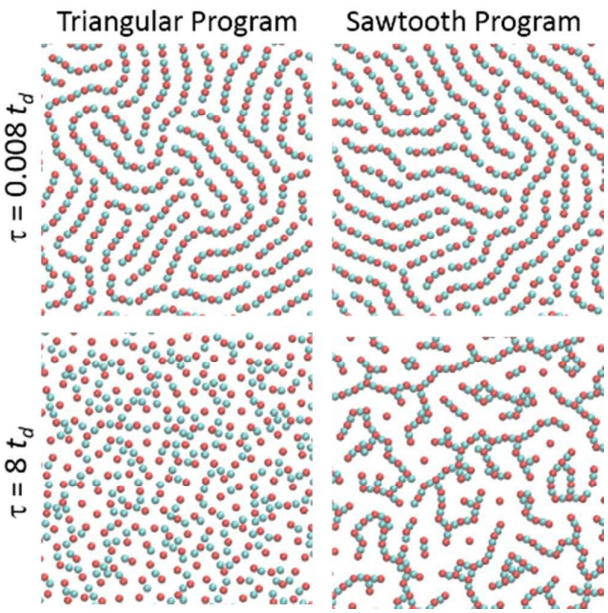

Figure 4: Simulation snapshots at a simulation time of 4 t_d for the same conditions of Figure 3.

Journal Name

View Article Online
DOI: 10.1039/C5FD00115C

Effect of the Frequency of pH Oscillations on the Dissipative Self-Assembly of Colloidal Molecules

The values of $\overline{\psi}_2$ in Figure 3 are maximal in the limit of very fast oscillations, $\tau \to 0$, i.e. fast oscillations favor the formation of well-order fibers. However, we show in this section that this conclusion is not general and that small oscillation frequencies can lead to more homogeneous mixtures of colloidal molecules than those obtained in the limit of very large frequencies.

As we mentioned above, when the pH is oscillated between 3 and 7, we only observe *a*, *b*, *ab* and a_2b particles (and ab_2 for systems rich in *b*-type particles). The effective potential allows us to assess the relative stability of each molecule in the system by calculating its potential energy in the limit of fast oscillations. Figure 5 shows the energy gain (or loss) upon formation of different colloidal molecules based on the effective potential. The predictions show that when the pH is oscillated from 3 to 7, the only stable a_ib colloidal molecules are *ab* and a_2b, in agreement with the simulation results. The rest of the colloidal molecules are unstable because in the effective potential, the *a*-*a* repulsions are stronger than the *a*-*b* attractions.[20] This situation changes by oscillating the pH from 3 to 5 (see Figure 1D), since in those conditions the charge of the *a*-type particles is (on average) smaller than that of the *b*-type particles. Therefore, *a*-*a* repulsions are weaker than *a*-*b* attractions and the latter are weaker than *b*-*b* repulsions. Figure 5 shows that when the pH is oscillated between 3 and 5, colloidal molecules with stoichiometries *ab*, a_2b, a_3b and a_4b can be obtained. Colloidal molecules with stoichiometries a_5b and a_6b have $U < 0$, but they are unstable with respect to the loss of satellite particles: breaking down a_5b particles into a_4b and *a* particles is energetically favourable.

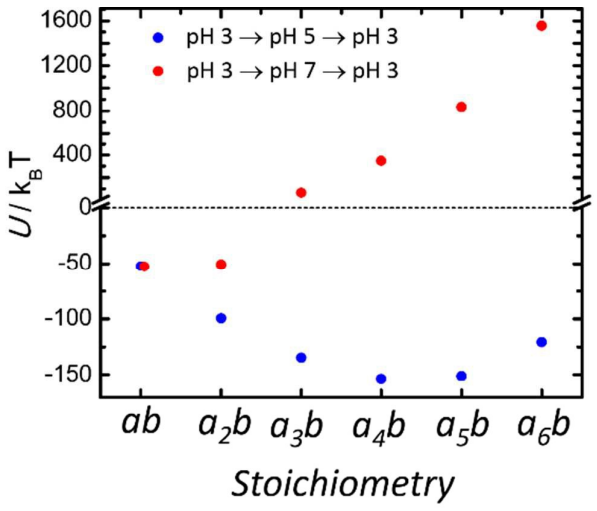

Figure 5: Potential energy of a_ib colloidal molecules determined in the limit $\tau \to 0$ with the effective potential, when the pH was oscillated with a triangular program between 3 and 7 (red points, pH program in Figure 1B) or between 3 and 5 (blue points, pH program in Figure 1D).

We estimated the population of each colloidal molecule in the NESS as a function of the density ρ and composition *a*:*b* using the energies in Figure 5 (see details in the Supporting Information). The calculation was done assuming equilibrium statistical mechanics with the effective potentials, since in the fast oscillation limit we have proven that to be the proper description.[20] Table 1 shows the predicted fractions, $f^p(a_ib)$, which we define as the number of particles in the system that belongs to a colloidal molecule with composition a_ib. We observe that for compositions 1:1, 2:1 and 3:1, the predicted stoichiometry of the predominant molecules is the same as the global composition of the system, while for 9:1, our calculations predict a mixture of isolated *a* particles and a_4b colloidal molecules because a_5b and a_6b particles are unstable.

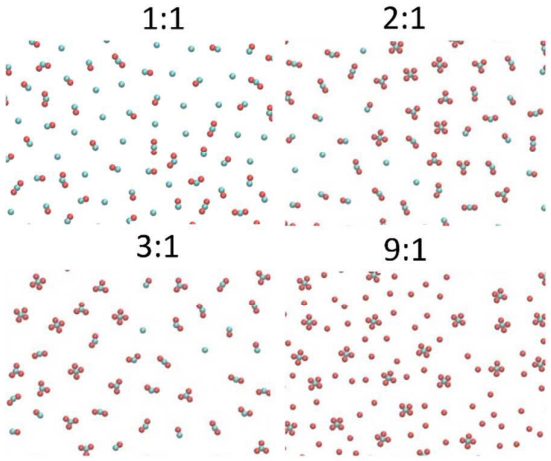

Figure 6. Snapshots showing the colloidal molecules formed in simulations where the pH was oscillated between 3 and 5 (program in Figure 1D), for $\tau \to 0$, $\rho = 0.11$ *part*·σ^{-2} and different *a*:*b* compositions. The fractions of each type of colloidal molecule for each different composition are summarized in Table 2

Figure 6 shows snapshots for simulations where the pH was oscillated between 3 and 5 in the limit of high frequencies, for $\rho = 0.11$ *part*·σ^{-2} and different compositions *a*:*b*. In all cases, we observe mixtures of different colloidal molecules. Table 2 shows the fractions of the different colloidal molecules in the systems of Figure 6. The populations of colloidal molecules predicted using the potential energy of the molecules (Table 1) and those actually observed in the simulations (Table 2) are very different. In the simulations, we observe a broad distribution of stoichiometries, while energetic arguments predict that almost all colloidal molecules should have a stoichiometry equal to the global composition of the system. This discrepancy arises because the colloidal molecules form within the first 1-3 t_d of simulation time (we start from a disordered system) and, after that time, particles cannot be exchanged between colloidal molecules. The fraction of each colloidal molecule in the system is, therefore, dictated by its formation kinetics during the initial stage of the simulation. This result means that for fast pH oscillations the system gets trapped in a non-equilibrium steady-state other than the most stable one, exactly in the same way as an

ARTICLE
View Article Online
Journal Name
DOI: 10.1039/C5FD00115C

equilibrium system can get trapped in a local (rather than the global) minimum of free-energy.

Table 1: Fraction of particles in the system that belong to colloidal molecules of different stoichiometries, $f^{p}(a_ib)$ for ρ = 0.11 *part*·σ^{-2} and different *a*:*b* compositions calculated from the potential energy of each molecule (see Supporting Information). The fractions of a_5b y a_6b is zero in all cases.

a:*b*	*a*	*b*	*ab*	a_2b	a_3b	a_4b
1:1	0.00	0.03	0.87	0.10	0.00	0.00
2:1	0.00	0.00	0.00	0.99	0.00	0.00
3:1	0.00	0.00	0.00	0.00	1.00	0.00
9:1	0.50	0.00	0.00	0.00	0.00	0.50

Table 2: Fraction of particles in the system that belong to colloidal molecules of different stoichiometries, $f^{p}(a_ib)$ obtained from simulations for ρ = 0.11 *part*·σ^{-2} and different *a*:*b* compositions in the limit τ→0 (see Figure 6). The fractions of a_5b y a_6b is zero in all cases.

a:*b*	*a*	*b*	*ab*	a_2b	a_3b	a_4b
1:1	0.00	0.17	0.40	0.32	0.11	0.00
2:1	0.00	0.03	0.18	0.30	0.33	0.16
3:1	0.02	0.01	0.05	0.16	0.29	0.47
9:1	0.47	0.00	0.03	0.01	0.00	0.47

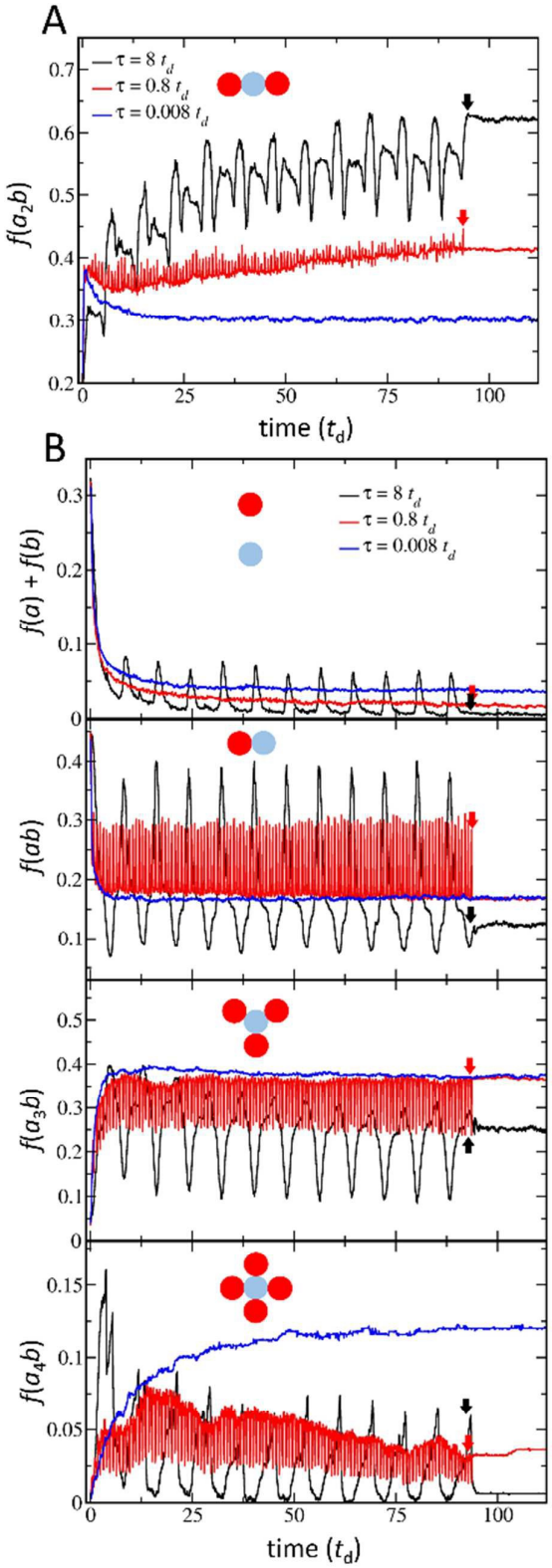

Figure 7: Fraction of the particles in the system that belong to a_ib colloidal molecules, $f^{p}(a_ib)$, as a function of the simulation time for different values of the oscillation period, τ and pH oscillations between 3 and 5 (pH program in Figure 1D). At the simulation times indicated with arrows, the period of pH oscillations was switched to τ = 0.008 t_d. Other simulation conditions: *a*:*b* = 2:1, *C* = 1000 k_BT·σ and ρ = 0.11 *part*·σ^{-2}.

Journal Name

View Article Online
ARTICLE
DOI: 10.1039/C5FD00115C

So far, we have shown that the effective potential allows to determine the conditions required to form dissipative self-assembled colloidal molecules, but it does not provide a way to avoid the kinetic traps that prevent the system from reaching its most stable NESS. We show next that these kinetic traps can be partially removed by the appropriate choice of the pH-oscillation period. In Figure 7A we plot the time course of the fraction of particles that belong to a_2b molecules in a system with a:b = 2:1 and ρ = 0.11 $part\cdot\sigma^{-2}$ for oscillations periods of 0.008, 0.8 and 8 t_d. For τ = 0.8 and 8 t_d, $f(a_2b)$ oscillates due to the oscillations of pH, but its value averaged over one period in the NESS (0.43 for τ = 0.8 t_d and 0.57 for τ = 8 t_d) is clearly larger than the value observed for very fast oscillations (0.30 for τ = 0.008 t_d). Inspection of the simulations shows that decreasing the oscillation period allows the exchange of a-type particles between colloidal molecules. Particle exchange occurs because a-type are almost neutral for pH = 3 and therefore at that pH there is no net a-b attraction. For very fast pH oscillations, a-type particles at pH 3 cannot diffuse fast enough to travel from one colloidal molecule to other before the pH changes. Note that electrostatic interactions in our system are rather strong (we used C = 1000 $k_bT\cdot\sigma$ in eq. (5)), therefore breaking the electrostatic bonds is very difficult if both a-type and b-type particles are charged. As the oscillation frequency decreases, the particles become able to escape from their original colloidal molecule, diffuse and attach to a different colloidal assembly. In the case of a 2:1 mixture, this process leads to a neat formation of a_2b molecules, which is the expected product according the energetics of the system, see Table 1.

For τ = 8 t_d, the fraction of a_2b particles displays large oscillations in time. In an attempt to maximize $f(a_2b)$, we switched the oscillation period from τ = 0.8 or 8 t_d to τ = 0.008 t_d when $f^p(a_2b)$ passed through a maximum. Figure 7A shows that $f^p(a_2b)$ remains stable after switching to fast oscillations (the switching times are shown with arrows). Figures 7B show the time evolution of the fraction of particles for the colloidal molecules different than a_2b. The increase of $f^p(a_2b)$ as the oscillation period increases is accompanied by a decrease in the fraction of the other colloidal molecules, especially free a-type, free b-type and a_4b particles, which drop to almost zero for τ = 8 t_d.

Figure 8 shows a plot of the final fraction of a_2b particles as a function of the period of the oscillations. We observe that $f^p(a_2b)$ increases up to $\tau \sim 8$ t_d and then remains constant (our data is noisy for large τ, for which the pH only oscillates a few times during the simulation). In the critical time scale of $t \sim 8$ t_d, a particle can diffuse an average distance of $(4Dt)^{1/2}$ = 5.7 σ. This distance agrees well with the average distance between colloidal molecules (estimated from the number of colloidal molecules and the area of the simulation box) of 5.2 σ, which confirms that the rate of a_2b formation is limited by the ability of a-type particles to exchange between colloidal molecules. It is also interesting to note that $f(a_2b)$ saturates around 0.63. In order to understand why larger $f(a_2b)$ cannot obtained, we show in Figure 9 snapshots of the system at the end of the simulation (112 t_d) for τ = 0.008 and 8 t_d. Molecules of different stoichiometry are shown in different colors. For τ = 8 t_d, the system is mainly composed by ab, a_2b and a_3b molecules. These three types of molecules are not homogeneously distributed, instead we observe regions rich in ab assemblies and other regions rich in a_3b colloids. The presence of regions that have different local compositions, which form due to random fluctuations during the initial assembly process, is the reason that prevents complete conversion to a_2b in the time scale of the simulation: a low oscillation frequency allows particles to exchange within colloidal molecules in a region, but it cannot eliminate longer-range heterogeneities of local composition.

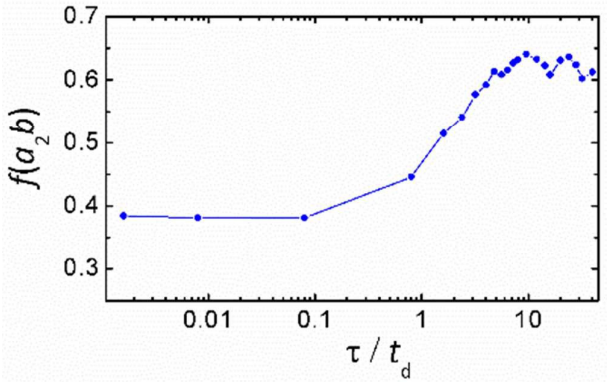

Figure 8: Fraction of a_2b colloidal molecules at the end of the simulation as a function of the oscillation period.

ARTICLE
View Article Online
Journal Name
DOI: 10.1039/C5FD00115C

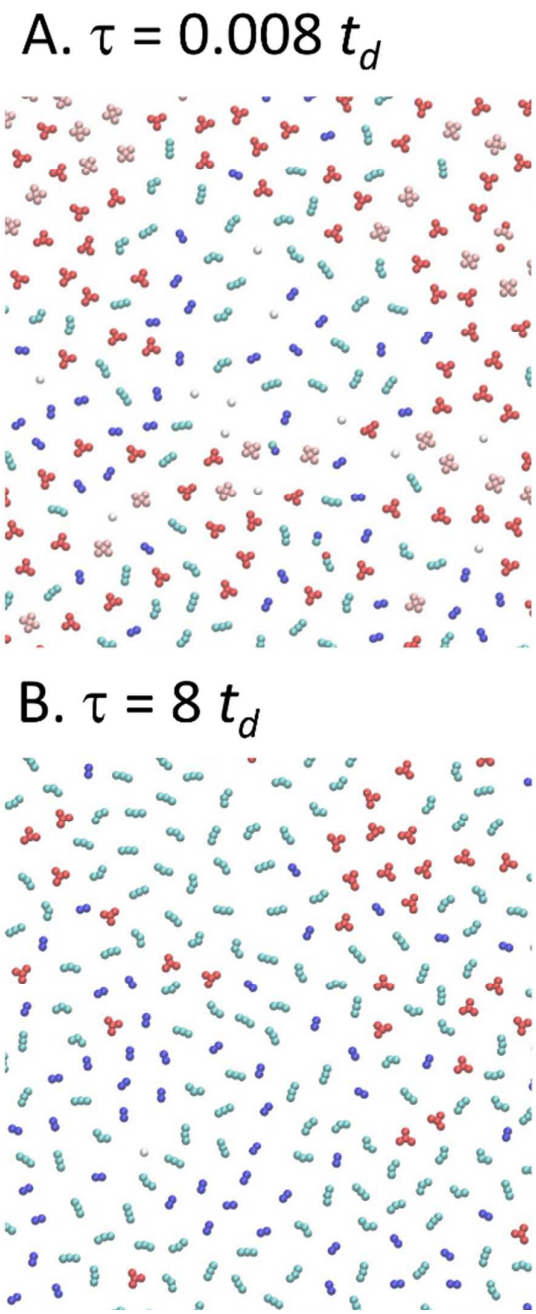

Figure 9: Simulation snapshots at t = 112 t_d for the simulation of Figure 7. A quarter of the simulation box (~ 625 particles) is shown in each panel. The particles are colored according to their stoichiometry: white for isolated a and b particles, blue for ab, cyan for a_2b, red for a_3b and pink for a_4b.

The results presented in this section show that slow pH oscillations can produce more ordered systems than fast oscillations. This result is applicable to the formation of colloidal molecules in systems with compositions different from 2:1, for example Figure 10 shows results for a system with a 3:1 composition. In this case, slow frequencies favor de formation of a_3b assemblies, which is the expected stoichiometry considering the global composition of the system. Moreover, our results are consistent with work in literature on the self-assembly of particles interacting through oscillatory forces. For example, Swan *et al*. studied the self-assembly of a magnetorheological fluid in the present of a toggling magnetic fields, whose oscillations allow the particles in the system to escape kinetic traps and form ordered structures.[34, 35] Simulations by Jha *et al*.[31] and Risbud *et al*.[32] studied the crystallization of particles whose interactions were turned on and off periodically and showed that there is an optimal and finite switching period that maximizes long-range order in the system. A common strategy that allows systems to jump over potential barrier, used in equilibrium systems, is to increase temperature. Periodically modulating the potential of the system also allows to jump over potential barriers, but it grants greater control over the final product than increasing the global temperature. A temperature jump increases the kinetic energy of the whole system, while changing the frequency of the oscillations provides for control of the length that a particle can diffuse and what are the initial and final states that the changing potentials provide. Thus, as a general conclusion, it is worthwhile to stress the role of the oscillation period as a handle to control the outcome of a dissipative self-assembly process. This handle has no equilibrium counterpart, which reinforces the idea that future synthetic dissipative systems may exhibit abilities for dynamical response and error correction well beyond the potential of equilibrium self-assembly.

Journal Name

View Article Online
ARTICLE
DOI: 10.1039/C5FD00115C

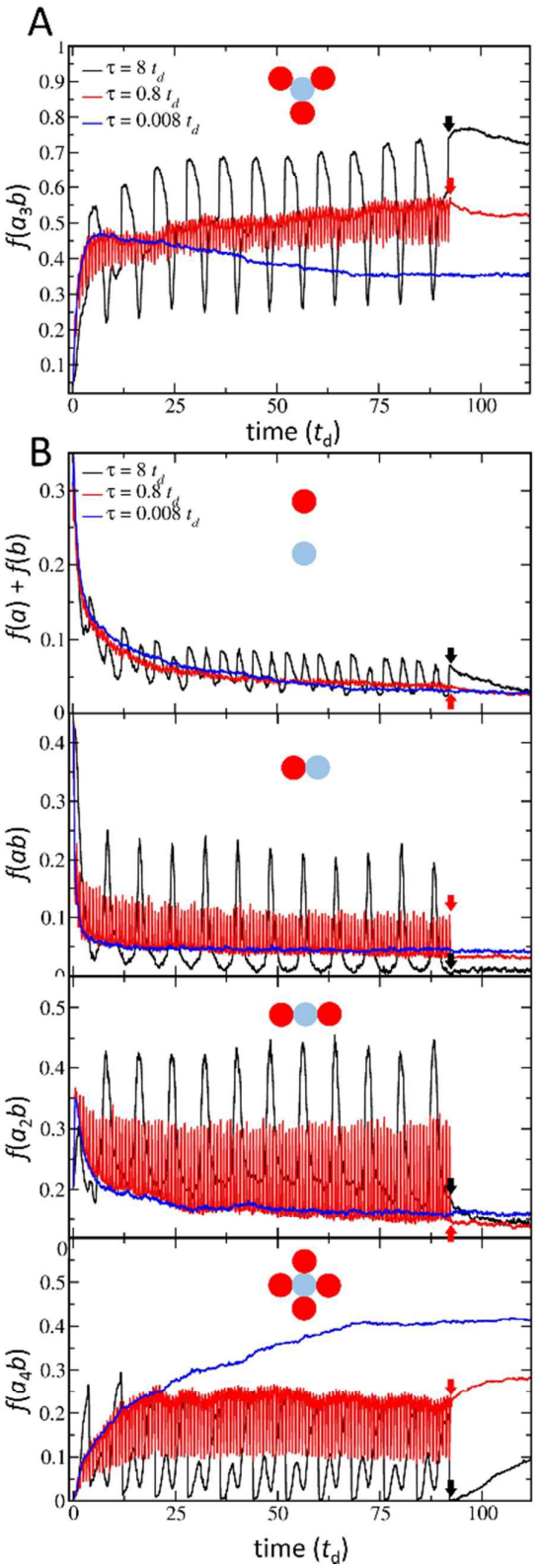

Figure 10: Same as Figure 7 for *a*:*b* = 3:1

Conclusions

In this work, we examined the dynamics of a dissipative system as it evolved toward a non-equilibrium steady-state. We demonstrate two important results. First, we showed using analytical theory and exemplified with numerical simulations that the whole dynamics of systems with time-oscillating interparticle potentials can be described, in the limit of fast oscillations, by an effective time-independent potential. This effective potential is the time average of the oscillatory potential. Dissipative systems may exhibit more than one non-equilibrium steady-state, for example magnetic spinners on the air-water interface may arrange in different patterns, each one corresponding to a different steady-state.[16, 38] It is unknown which of these steady-states is the most stable one or if it is even correct to think as one of them as being more stable than the others. In the particular case of particles interacting through fast oscillatory forces, we solved this problem by demonstrating the existence of an effective potential, which maps the non-equilibrium problem into an equilibrium one. This result allows applying the tools of equilibrium thermodynamics to the study of dissipative systems. For example, we used the effective potential to calculate the energy of colloidal molecules of different stoichiometries and then applied the tools of equilibrium statistical mechanics to calculate the fraction of each of these molecules in the (most stable) non-equilibrium steady-state of the system.

The second important result of the present paper is related to the effect of the oscillation period on the formation of order. We observed that in some cases (i.e. formation of fibers), ordered structures are favored by fast oscillations, while in others (formation of colloidal molecules) slow oscillations increase the order of the system by allowing it to escape from kinetic traps. Previous works have shown that oscillating interparticle forces can assist the crystallization of colloids.[31, 32, 34] Our results on colloidal molecules are related to these effects previously reported in the literature, with the difference that in previous works the colloidal crystals were an equilibrium product of the system (and the oscillations were introduced as perturbations), while in our case the colloidal molecules are dissipative structures that cannot be obtained in the absence of pH oscillations. The efficiency of trap removal by oscillating interparticle forces will, of course, depend on the details of the interparticle potential and should probably be analyzed on a case-per-case basis.

We arrived to the conclusions mentioned in the previous paragraphs by analyzing a system of particles coated by weak acids and bases under pH oscillations. This system is appealing to study dissipative self-assembly due to the richness of structures that it produces as well as its chemical relevance. However, our conclusion about the existence of a non-oscillatory potential that describes the dynamics of particles interacting through oscillatory forces is valid for any oscillatory potential. We believe that this conclusion also applies to systems under oscillating external fields and we will analyze this case in the future. Our work exemplifies two interesting

ARTICLE
View Article Online
Journal Name
DOI: 10.1039/C5FD00115C

aspects of dissipative self-assembly that are unavailable to equilibrium self-assembly: i) the effective potential depends on the how of the interparticle potential is oscillated in time (e.g. the shape of the pH-time program). This dependence provides a dynamic handle to engineer the interactions among particles that is unique to dissipative systems, ii) the oscillations play the dual role of controlling the effective potential among particles and of removing kinetic traps, which results in an unique ability of dissipative systems of avoiding kinetically arrested states and provides a potential avenue for self-healing and error correction.

Acknowledgements

This work was supported as part of the Center for Bio-Inspired Energy Science, an Energy Frontier Research Center funded by the U.S. Department of Energy, Office of Science, Basic Energy Sciences, under Award no. DE-SC0000989. This research was supported in part through the computational resources and staff contributions provided by the Quest high performance computing facility at Northwestern University which is jointly supported by the Office of the Provost, the Office for Research, and Northwestern University Information Technology. MT is a fellow of CONICET (Argentina).

Notes and references

1. G. Van Anders, D. Klotsa, N. K. Ahmed, M. Engel and S. C. Glotzer, *Proceedings of the National Academy of Sciences of the United States of America*, 2014, **111**, E4812-E4821.
2. N. R. Jana, *Angewandte Chemie - International Edition*, 2004, **43**, 1536-1540.
3. X. Ye, J. E. Collins, Y. Kang, J. Chen, D. T. N. Chen, A. G. Yodh and C. B. Murray, *Proceedings of the National Academy of Sciences of the United States of America*, 2010, **107**, 22430-22435.
4. Y. Wang, Y. Wang, D. R. Breed, V. N. Manoharan, L. Feng, A. D. Hollingsworth, M. Weck and D. J. Pine, *Nature*, 2012, **491**, 51-55.
5. Q. Chen, S. C. Bae and S. Granick, *Nature*, 2011, **469**, 381-384.
6. Q. Chen, E. Diesel, J. K. Whitmer, S. C. Bae, E. Luijten and S. Granick, *Journal of the American Chemical Society*, 2011, **133**, 7725-7727.
7. P. F. Damasceno, M. Engel and S. C. Glotzer, *Science*, 2012, **337**, 453-457.
8. A. Bricard, J.-B. Caussin, N. Desreumaux, O. Dauchot and D. Bartolo, *Nature*, 2013, **503**, 95-98.
9. M. Tagliazucchi, F. Zou and E. A. Weiss, *Journal of Physical Chemistry Letters*, 2014, **5**, 2775-2780.
10. J. A. Balmer, O. O. Mykhaylyk, J. Patrick A Falrclough, A. J. Ryan, S. P. Armes, M. W. Murray, K. A. Murray and N. S. J. Williams, *Journal of the American Chemical Society*, 2010, **132**, 2166-2168.
11. X. Mao, Q. Chen and S. Granick, *Nature Materials*, 2013, **12**, 217-222.
12. M. D. Eldridge, P. A. Madden and D. Frenkel, *Nature*, 1993, **365**, 35-XI.
13. W. M. Jacobs, A. Reinhardt and D. Frenkel, *Proceedings of the National Academy of Sciences of the United States of America*, 2015, **112**, 6313-6318.
14. B. De Nijs, S. Dussi, F. Smallenburg, J. D. Meeldijk, D. J. Groenendijk, L. Filion, A. Imhof, A. Van Blaaderen and M. Dijkstra, *Nature Materials*, 2015, **14**, 56-60.
15. D. Helbing, I. J. Farkas and T. Vicsek, *Physical Review Letters*, 2000, **84**, 1240-1243.
16. B. A. Grzybowski, H. A. Stone and G. M. Whitesides, *Nature*, 2000, **405**, 1033-1036.
17. R. Klajn, K. J. M. Bishop and B. A. Grzybowski, *Proceedings of the National Academy of Sciences of the United States of America*, 2007, **104**, 10305-10309.
18. M. E. Leunissen, C. G. Christova, A. P. Hynninen, C. P. Royall, A. I. Campbell, A. Imhof, M. Dijkstra, R. van Roij and A. van Blaaderen, *Nature*, 2005, **437**, 235-240.
19. N. H. P. Nguyen, D. Klotsa, M. Engel and S. C. Glotzer, *Physical Review Letters*, 2014, **112**.
20. M. Tagliazucchi, E. A. Weiss and I. Szleifer, *Proc Natl Acad Sci USA* 2014, **DOI: 10.1073/pnas.1406122111**.
21. R. Ni, M. A. C. Stuart and M. Dijkstra, *Nat Commun*, 2013, **4**.
22. D. K. Kim, Y. Lai, B. T. Diroll, C. B. Murray and C. R. Kagan, *Nature Communications*, 2012, **3**.
23. W.-k. Koh, S. R. Saudari, A. T. Fafarman, C. R. Kagan and C. B. Murray, *Nano Letters*, 2011, **11**, 4764-4767.
24. H. Zhang, X. Yu and P. V. Braun, *Nature Nanotechnology*, 2011, **6**, 277-281.
25. S. A. McDonald, G. Konstantatos, S. Zhang, P. W. Cyr, E. J. D. Klem, L. Levina and E. H. Sargent, *Nature Materials*, 2005, **4**, 138-142.
26. D. J. Park, C. Zhang, J. C. Ku, Y. Zhou, G. C. Schatz and C. A. Mirkin, *Proceedings of the National Academy of Sciences of the United States of America*, 2015, **112**, 977-981.
27. R. A. Alvarez-Puebla, A. Agarwal, P. Manna, B. P. Khanal, P. Aldeanueva-Potel, E. Carbó-Argibay, N. Pazos-Pérez, L. Vigderman, E. R. Zubarev, N. A. Kotov and L. M. Liz-Marzán, *Proceedings of the National Academy of Sciences of the United States of America*, 2011, **108**, 8157-8161.
28. M. Fialkowski, K. J. M. Bishop, R. Klajn, S. K. Smoukov, C. J. Campbell and B. A. Grzybowski, *Journal of Physical Chemistry B*, 2006, **110**, 2482-2496.
29. K. Yeo, E. Lushi and P. M. Vlahovska, *Physical Review Letters*, 2015, **114**.
30. N. H. P. Nguyen, E. Jankowski and S. C. Glotzer, *Physical Review E*, 2012, **86**.
31. P. K. Jha, V. Kuzovkov, B. A. Grzybowski and M. Olvera de la Cruz, *Soft Matter*, 2012, **8**, 227-234.
32. S. R. Risbud and J. W. Swan, *Soft Matter*, 2015, **11**, 3232-3240.
33. J. R. Green, A. B. Costa, B. A. Grzybowski and I. Szleifer, *Proceedings of the National Academy of Sciences of the United States of America*, 2013, **110**, 16339-16343.
34. J. W. Swan, P. A. Vasquez, P. A. Whitson, E. M. Fincke, K. Wakata, S. H. Magnus, F. De Winne, M. R. Barratt, J. H. Agui, R. D. Green, N. R. Hall, D. Y. Bohman, C. T. Bunnell, A. P. Gast and E. M. Furst, *Proceedings of the National Academy of Sciences of the United States of America*, 2012, **109**, 16023-16028.
35. J. W. Swan, J. L. Bauer, Y. Liu and E. M. Furst, *Soft Matter*, 2014, **10**, 1102-1109.

View Article Online
ARTICLE
DOI: 10.1039/C5FD00115C

36. J. Yan, M. Bloom, S. C. Bae, E. Luijten and S. Granick, *Nature*, 2012, **491**, 578-581.
37. J. E. Martin and A. Snezhko, *Reports on Progress in Physics*, 2013, **76**.
38. K. V. Tretiakov, I. Szleifer and B. A. Grzybowski, *Angewandte Chemie - International Edition*, 2013, **52**, 10304-10308.
39. D. W. Wang, R. J. Nap, I. Lagzi, B. Kowalczyk, S. B. Han, B. A. Grzybowski and I. Szleifer, *Journal of the American Chemical Society*, 2011, **133**, 2192-2197.
40. M. Tagliazucchi and I. Szleifer, *Soft Matter*, 2012, **8**, 7292-7305.
41. B. W. Ninham and A. Parsegian, *Journal of Theoretical Biology*, 1971, **31**, 405-&.
42. W. Coffey, *The Langevin equation : with applications to stochastic problems in physics, chemistry, and electrical engineering*, World Scientific, River Edge, NJ, 3rd ed.. edn., 2012.
43. J. Dobnikar, Y. Chen, R. Rzehak and H. H. Von Grünberg, *Journal of Physics Condensed Matter*, 2003, **15**, S263-S268.
44. W. Lechner and C. Dellago, *Journal of Chemical Physics*, 2008, **129**.
45. R. Zhang, P. K. Jha and M. Olvera de La Cruz, *Soft Matter*, 2013, **9**, 5042-5051.
46. D. R. Nelson and B. I. Halperin, *Physical Review B*, 1979, **19**, 2457-2484.